

# CENTRAL ENGINES DIE YOUNG IN RELATIVISTIC SUPERNOVAE: THE CASE OF SN 2012AP

R. MARGUTTI<sup>1</sup>, D. MILISAVLJEVIC<sup>1</sup>, A. M. SODERBERG<sup>1</sup>, C. GUIDORZI<sup>2</sup>, B. J. MORSONY<sup>3</sup>, N. SANDERS<sup>1</sup>, S. CHAKRABORTI<sup>1</sup>, A. RAY<sup>5</sup>, A. KAMBLE<sup>1</sup>, M. DROUT<sup>1</sup>, J. PARRENT<sup>1</sup>, A. ZAUDERER<sup>1</sup>, L. CHOMIUK<sup>4</sup>

*Draft version February 27, 2014*

## ABSTRACT

Deep late-time X-ray observations of the relativistic, engine-driven, Type Ic SN 2012ap allow us to probe the nearby environment of the explosion and reveal the unique properties of relativistic SNe. We find that on a local scale of  $\sim 0.01$  pc the environment was shaped directly by the evolution of the progenitor star with a pre-explosion mass-loss rate  $\dot{M} < 5 \times 10^{-6} M_{\odot} \text{ yr}^{-1}$ , in line with GRBs and the other relativistic SN2009bb. Like sub-energetic GRBs, SN 2012ap is characterized by a bright radio emission and evidence for mildly relativistic ejecta. However, its late time ( $\delta t \approx 20$  d) X-ray emission is  $\sim 100$  times fainter than the faintest sub-energetic GRB at the same epoch, with no evidence for late-time central engine activity. Our results suggest that relativistic SNe like 2009bb and 2012ap represent the weakest engine-driven explosions, where the engine is unable to power a successful jet breakout. This phenomenology can either be due to an intrinsically short-lived engine or to different progenitor properties between relativistic SNe and GRBs.

*Subject headings:* supernovae: specific (SN 2012ap); GRBs

## 1. INTRODUCTION

The vast majority of supernova explosions (SNe) arising from hydrogen and helium stripped progenitors (i.e. Type Ic SNe) can be explained by the hydrodynamical collapse of the massive progenitor star (e.g. Tan et al. 2001). In a very limited percentage of cases ( $\lesssim 1\%$ , Guetta & Della Valle 2007, Soderberg et al. 2010b), the explosion is instead powered by an engine able to accelerate a tiny portion of the ejecta with typical mass<sup>6</sup>  $M \approx 10^{-5} - 10^{-6} M_{\odot}$  to velocities  $v \gtrsim 0.6c$ . Engine-driven explosions (E-SNe hereafter) are thus uncommon. Only a small fraction of E-SNe ( $\approx 10\%$ , e.g. Soderberg et al. 2006a) harbor a fully relativistic jet and give origin to Gamma-Ray Bursts (GRBs). The peculiar circumstances that cause an hydrogen-stripped, massive progenitor star to produce a relativistic jet at the time of the collapse are still not fully understood. High angular momentum seems to be a key ingredient (e.g. MacFadyen & Woosley 1999, MacFadyen et al. 2001, Woosley & Heger 2006, Dessart et al. 2008).

E-SNe have historically been detected through their prompt X-ray and  $\gamma$ -ray emission produced by energy dissipation within the jet (ordinary GRBs) and by the SN shock breakout (which is relevant for some sub-energetic -sub-E- GRBs, e.g. Campana et al. 2006; Bromberg et al. 2011; Nakar & Sari 2012). More recently, two E-SNe have been discovered through their bright later-time radio emission (i.e. the relativistic SNe 2009bb and 2012ap, Soderberg et al. 2010b, Chakraborti et al., 2014, hereafter C14). PTF11agg might be the first example of cosmological burst detected through its optical emission without a high-energy trigger (Cenko et al.

2013).

Relativistic SNe 2009bb and 2012ap share with sub-E GRBs evidence for mildly relativistic ejecta powering a bright radio emission and a very energetic optical explosion with  $E_k \sim 10^{52}$  erg coupled to slowly moving material ( $v \sim$  a few  $10^4 \text{ km s}^{-1}$ ). These properties dynamically distinguish relativistic SNe and sub-E GRBs from ordinary SNe, and put these explosions between the highly-relativistic, collimated GRBs and the more common Type Ic SNe (see e.g. Soderberg et al. 2006a, 2010b, C14).

Here we present late-time, deep X-ray observations of SN 2012ap. These observations allow us to identify a key property of relativistic SNe: compared with sub-E GRBs, relativistic SNe show a significantly fainter X-ray emission (SN 2012ap is  $\sim 100$  times fainter than the faintest sub-E GRB at the same epoch). We interpret this finding in the context of state-of-the art simulations of jet-driven stellar explosions (Lazzati et al. 2012) and suggest that relativistic SNe represent the weakest engine-driven explosions, where the engine is short lived and unable to power a successful jet breakout. Classic GRBs are instead associated with fully-developed, highly-relativistic jets. Sub-E GRBs likely represent an intermediate case, where the jet is just barely able to pierce through the stellar envelope, the central engine is longer-lived and is responsible for the late-time ( $\delta t > 10$  d) excess of X-ray radiation recently reported for the sub-E GRBs 060218 (Soderberg et al. 2006a; Fan & Piran 2006) and 100316D (Margutti et al. 2013a).

This paper is organized as follows. X-ray observations are described in Sec. 2. We use these observations to derive a limit to the mass-loss rate of the stellar progenitor of SN 2012ap in the years before the terminal explosion in Sec. 3. We analyze and discuss the properties of SN 2012ap in the context of engine-driven explosions in Sec. 4 and 5. Conclusions are drawn in Sec. 6.

Uncertainties are quoted at  $1\sigma$  confidence level, unless otherwise noted. We employ standard cosmology with  $H_0 = 71 \text{ km s}^{-1} \text{ Mpc}^{-1}$ ,  $\Omega_{\Lambda} = 0.73$ , and  $\Omega_M = 0.27$ . Throughout the paper we use 2012 February 5th as the explosion date of SN 2012ap, as inferred by Milisavljevic et al., in prep. (M14,

<sup>1</sup> Harvard-Smithsonian Center for Astrophysics, 60 Garden St., Cambridge, MA 02138, USA

<sup>2</sup> Department of Physics and Earth Sciences, University of Ferrara, via Saragat 1, I-44122, Ferrara, Italy

<sup>3</sup> Department of Astronomy, University of Wisconsin-Madison, 2535 Sterling Hall, 475 N. Charter Street, Madison WI 53706 -1582, USA

<sup>4</sup> Department of Physics and Astronomy, Michigan State University, East Lansing, MI 48824, USA

<sup>5</sup> Department of Astronomy and Astrophysics, Tata Institute of Fundamental Research, 1 Homi Bhabha Road, Mumbai 400 005, India

<sup>6</sup> For the relativistic SN 2009bb  $M \approx 10^{-2} M_{\odot}$  (Chakraborti & Ray 2011).

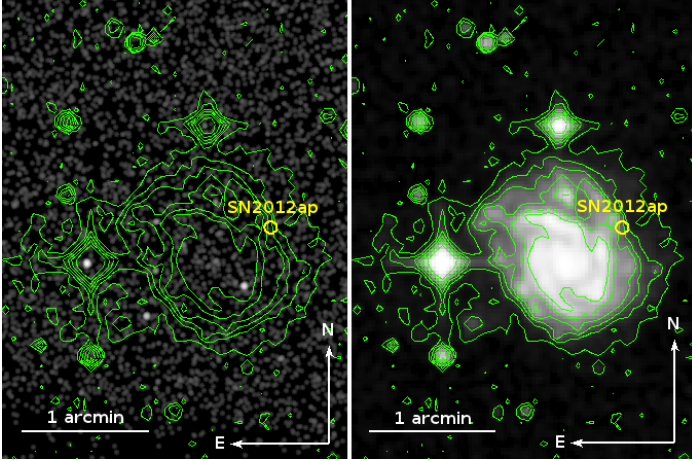


FIG. 1.— X-ray (*Chandra*, 0.5-8 keV, left panel) and pre-explosion optical image (SDSS, right panel) of the region around SN 2012ap. No X-ray emission is detected at the position of SN 2012ap at  $\delta t \approx 24$  d after the explosion down to a deep luminosity limit of  $L_x \sim 2 \times 10^{39} \text{ erg s}^{-1}$  (0.3-10 keV). Yellow circle:  $2''$  radius region around SN 2012ap. Optical contours have been overlaid to the X-ray image for reference.

hereafter) from extensive optical observations. Following C14 we assume a distance of 40 Mpc (Springob et al. 2007, 2009). A detailed discussion of the optical and radio properties of SN 2012ap can be found in M14 and C14, respectively.

## 2. OBSERVATIONS AND DATA ANALYSIS

### 2.1. *Swift*-XRT

We observed SN 2012ap with the *Swift* (Gehrels et al. 2004) X-ray Telescope (XRT, Burrows et al. 2005) starting from 2012 February 12th ( $\delta t \approx 7$  d) until March 2nd ( $\delta t \approx 26$  d). No X-ray source is detected at the position of SN 2012ap. Analyzing the XRT data using the latest HEASoft release (v6.13) and employing standard filtering and screening criteria, we determine a  $3\sigma$  count-rate upper limit to the X-ray emission from SN 2012ap of  $7.3 \times 10^{-4} \text{ cps}$  (0.3-10 keV energy band, total exposure time of 35 ks). The Galactic neutral hydrogen column density in the direction of SN 2012ap is  $N_H = 4.9 \times 10^{20} \text{ cm}^{-2}$  (Kalberla et al. 2005). The analysis of the optical spectra presented in Milisavljevic et al. (2014) constrains the intrinsic color excess towards SN 2012ap to be  $0.18 \text{ mag} < E(B-V) < 0.57 \text{ mag}$ . Using the Galactic relations between the extinction  $A_V$  and the  $N_H$  ( $N_{H,\text{int}}/A_V \approx (1.7 - 2.2) \times 10^{21} \text{ cm}^{-2}$ , Predehl & Schmitt 1995, Watson 2011), the limit on the color excess above translates into  $N_{H,\text{int}} < 3.9 \times 10^{21} \text{ cm}^{-2}$ . Assuming a simple power-law spectral model with photon index  $\Gamma = 2$ , the absorbed (unabsorbed) flux limit is  $F_x < 2.6 \times 10^{-14} \text{ erg s}^{-1} \text{ cm}^{-2}$  ( $F_x < 5.8 \times 10^{-14} \text{ erg s}^{-1} \text{ cm}^{-2}$ ), corresponding to a luminosity  $L_x < 1.1 \times 10^{40} \text{ erg s}^{-1}$  (0.3-10 keV) at the distance of 40 Mpc.

### 2.2. *Chandra*

We initiated deep X-ray follow up of SN 2012ap with the *Chandra* X-ray Observatory on 2012 Feb 29.2 UT,  $\delta t \approx 24$  d after the explosion (Program 13500648; PI Soderberg). *Chandra* ACIS-S data were reduced with the CIAO software package (v4.5) and relative calibration files, applying standard ACIS data filtering. Using *wavedetect* we find no evidence for X-ray emission at the position of SN 2012ap (Fig. 1), with a  $3\sigma$  limit of  $8.0 \times 10^{-4} \text{ cps}$  (0.5-8 keV energy range, total exposure time of 9.9 ks). Employing the

spectral parameters above, the corresponding absorbed (unabsorbed) flux limit in the 0.3-10 keV energy range is  $F_x < 6.8 \times 10^{-15} \text{ erg s}^{-1} \text{ cm}^{-2}$  ( $F_x < 1.3 \times 10^{-14} \text{ erg s}^{-1} \text{ cm}^{-2}$ ). The luminosity limit is  $L_x < 2.4 \times 10^{39} \text{ erg s}^{-1}$  (0.3-10 keV).

## 3. CONSTRAINTS TO THE PROGENITOR MASS-LOSS RATE

At  $\delta t \lesssim 30$  d Inverse Compton (IC) is the dominating X-ray emission mechanisms for ordinary SNe arising from hydrogen-stripped progenitors exploding in low density environments (Björnsson & Fransson 2004; Chevalier & Fransson 2006). In the case of central-engine powered SNe, additional sources of X-ray power are represented by continued central engine activity (as in the case of sub-E GRBs like 100316D, Margutti et al. 2013a) and interaction of the explosion jet with the environment (as in the case of ordinary GRBs, see e.g. Margutti et al. 2013b). In the following we use the deep *Chandra* limit of Sec. 2.2 and conservatively assume that IC is responsible for the entire X-ray emission to derive a solid upper limit to the mass-loss rate of the progenitor star of SN 2012ap.

In the IC scenario the X-ray emission is originated by up-scattering of optical photons from the SN photosphere by a population of relativistic electrons and depends on: (i) the density structure of the SN ejecta (ii) and of the circum-stellar medium (CSM); (iii) the details of the electron distribution responsible for the up-scattering; (iv) the explosion parameters (ejecta mass  $M_{\text{ej}}$  and kinetic energy<sup>7</sup>  $E_k$ ); and (v) the bolometric luminosity of the SN:  $L_{\text{IC}} \propto L_{\text{bol}}$ . We adopt the formalism by Margutti et al. (2012) modified to account for the outer density structure of SNe with compact progenitors that has been shown to scale as  $\rho_{\text{SN}} \propto R^{-n}$  with  $n \sim 10$  (see e.g. Matzner & McKee 1999; Chevalier & Fransson 2006).

Assuming a wind-like CSM structure  $\rho_{\text{CSM}} \propto R^{-2}$  as appropriate for massive stars, a power-law electron distribution  $n_e(\gamma) = n_0 \gamma^{-p}$  with  $p \sim 3$  as indicated by radio observations of type Ib/c SNe (Chevalier & Fransson 2006) and by radio observations of SN 2012ap (C14) and a fraction of energy into relativistic electrons  $\epsilon_e = 0.1$  as supported by well studied SN shocks (e.g. Chevalier & Fransson 2006), the *Chandra* non-detection of SN 2012ap at  $\delta t \approx 24$  d implies  $\dot{M}/v_w < 5 \times 10^{-6} (M_\odot \text{ y}^{-1} / 1000 \text{ km s}^{-1})$ .  $\dot{M}$  is the mass loss rate of the progenitor star and  $v_w$  is the wind velocity. We renormalize the mass-loss to  $v_w = 1000 \text{ km s}^{-1}$  as appropriate for a Wolf Rayet progenitor stars. In this calculation we used the bolometric luminosity we derived in M14,  $E_k \sim 10^{52} \text{ erg}$  and  $M_{\text{ej}} \sim 3 M_\odot$  as obtained by modeling the bolometric luminosity in M14.

The inferred limit to the mass-loss rate  $\dot{M} < 5 \times 10^{-6} (M_\odot \text{ y}^{-1})$  is independent from any assumption on magnetic-field related parameters, it is not affected by possible uncertainties on the SN distance and indicates that the pre-explosion mass-loss of SN 2012ap lies at the low end of the interval of values derived by C14 ( $4 \times 10^{-6} M_\odot \text{ y}^{-1} < \dot{M} < 5 \times 10^{-5} M_\odot \text{ y}^{-1}$ ) based on the modeling of the radio observations with synchrotron emission.<sup>8</sup> This result is in line with the value derived for the relativistic SN 2009bb ( $\dot{M} \sim 2 \times 10^{-6} M_\odot \text{ y}^{-1}$ , Soderberg et al. 2010b) and consistent with the wide range of values inferred for sub-E GRBs ( $10^{-7} M_\odot \text{ y}^{-1} \lesssim \dot{M} \lesssim 10^{-5} M_\odot \text{ y}^{-1}$ ).

<sup>7</sup> This is the kinetic energy carried by the slowly moving material powering the optical emission.

<sup>8</sup> Note that the synchrotron formalism is instead dependent on assumptions on magnetic field related parameters.

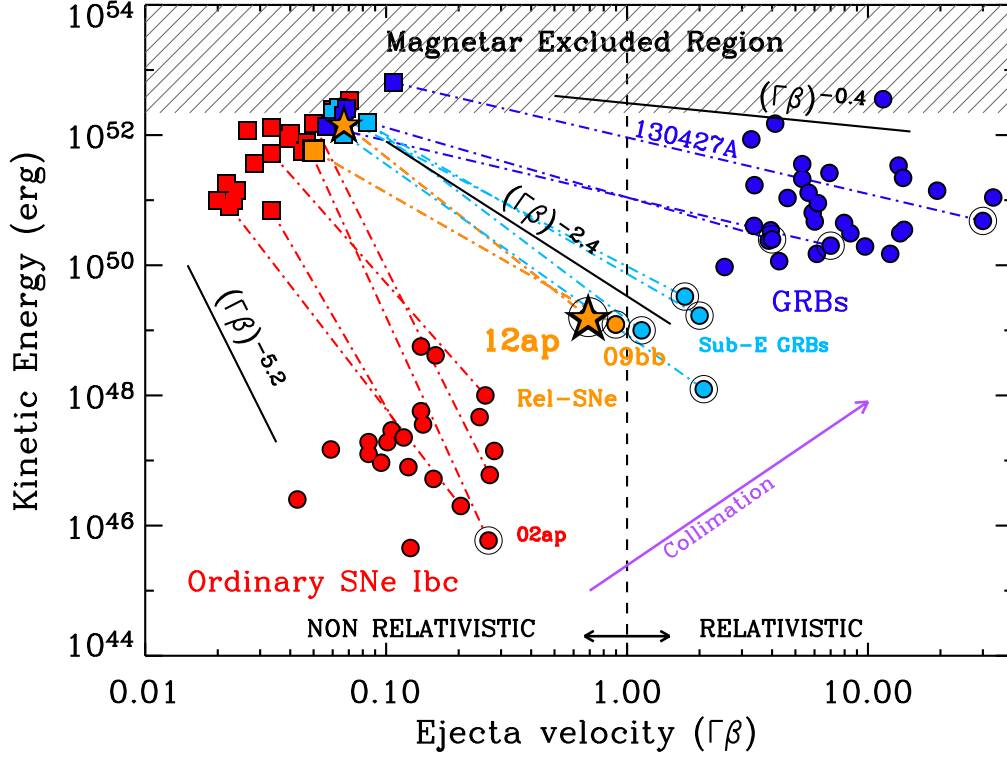


FIG. 2.— Kinetic energy profile of the ejecta of ordinary type Ibc SNe (red) and E-SNe, a class of explosions that includes GRBs (blue), sub-E GRBs (light-blue) and relativistic SNe (orange). Squares and circles are used for the slow-moving and the fast-moving ejecta, respectively, as measured from optical and radio observations. The velocity of the fast-moving ejecta has been computed at  $\delta t = 1$  d (rest-frame). Black solid lines: ejecta kinetic energy profile of a pure hydrodynamical explosion ( $E_k \propto (\Gamma\beta)^{-5.2}$ , Tan et al. 2001), and for explosions powered by a short-lived ( $E_k \propto (\Gamma\beta)^{-2.4}$ ) and long-lived ( $E_k \propto (\Gamma\beta)^{-0.4}$ ) central engine (Lazzati et al. 2012). Open black circles identify explosions with broad-lined optical spectra. The purple arrow identifies the direction of increasing collimation of the fastest ejecta. SN 2012ap bridges the gap between cosmological GRBs and ordinary SNe Ibc. Its kinetic energy profile, significantly flatter than what expected from a pure hydrodynamical explosion, indicates the presence of a central engine. References: Margutti et al. (2013a) and references therein; Horesh et al. (2013); C14; M14.

#### 4. SN 2012AP IN THE CONTEXT OF ENGINE-DRIVEN EXPLOSIONS

The radio observations of SN 2012ap are well modeled by synchrotron emission arising from the interaction of the SN shock with the environment (C14). C14 derive  $E_k = (1.6 \pm 0.1) \times 10^{49}$  erg carried by mildly relativistic ejecta with velocity  $v \sim 0.7c$  at  $\delta t = 1$  d. By modeling the observed optical emission, M14 infer  $E_k \sim 10^{52}$  erg in slow moving ( $v \approx 20000 \text{ km s}^{-1}$ ) material. These two values define an  $E_k$  profile significantly flatter than what expected in the case of a pure hydrodynamical collapse ( $E_k \propto (\Gamma\beta)^{-5.2}$ , e.g. Tan et al. 2001), thus pointing to the *presence of an engine driving the SN 2012ap explosion* (see Fig. 2).

Engine-driven SNe (E-SNe) constitute a diverse class of explosions that includes relativistic SNe, sub-E GRBs and ordinary GRBs. SN 2012ap is intermediate between ordinary non-relativistic SNe and fully relativistic GRBs and falls into a region of the parameter space populated by sub-E GRBs and the other known relativistic SN, SN 2009bb (Fig. 2)<sup>9</sup>. With reference to figures 3 and 4 we find that:

- The radio luminosity of SN 2012ap and sub-E GRBs is comparable. SN 2012ap is significantly more luminous than ordinary Ic SNe at the same epoch, and even more luminous than the sub-E GRBs 100316D and 060218 (Fig. 3, right panel). With  $E_k \sim 10^{52}$  erg and evi-

dence for broad spectral features (M14), the properties of SN 2012ap in the optical band are also reminiscent of the very energetic SNe associated with sub-E GRBs and ordinary GRBs.

- At  $\delta t \sim 20$  d, the X-ray emission from SN 2012ap is however a factor  $\geq 100$  fainter than the faintest sub-E GRB ever detected, GRB 980425 (Fig. 3, left panel).
- Along the same line, from C14, the prompt  $\gamma$ -ray energy released by the SN 2012ap explosion is  $E_{\gamma, \text{iso}} < 10^{47}$  erg, a factor  $\geq 10$  fainter than the faintest sub-E GRB 980425 (Fig. 4).

Relativistic SNe and sub-E GRBs are thus clearly distinguished in terms of their high-energy (X-rays and  $\gamma$ -rays) properties. The different level of X-ray emission between relativistic SNe and sub-E GRBs cannot be ascribed to beaming of collimated emission away from our line of sight. Radio observations of sub-E GRBs support the idea of quasi-spherical explosions (e.g. Soderberg et al. 2006a, Margutti et al. 2013a), while there is no evidence for beaming of the non-thermal emission from relativistic SNe (Soderberg et al. 2010b; C14). Furthermore, on a time scale of  $\sim 20$  d, the blastwave arising from both relativistic SNe and sub-E GRBs is sub-relativistic and the geometry of emission is effectively spherical, independent from the initial conditions. The different level of X-ray emission between sub-E GRBs and relativistic SNe at  $t \gtrsim 10$  d is thus intrinsic.

<sup>9</sup> The relativistic nature of SN 2007gr has been questioned by Soderberg et al. (2010a) and it is not included here. See however Paragi et al. (2010).

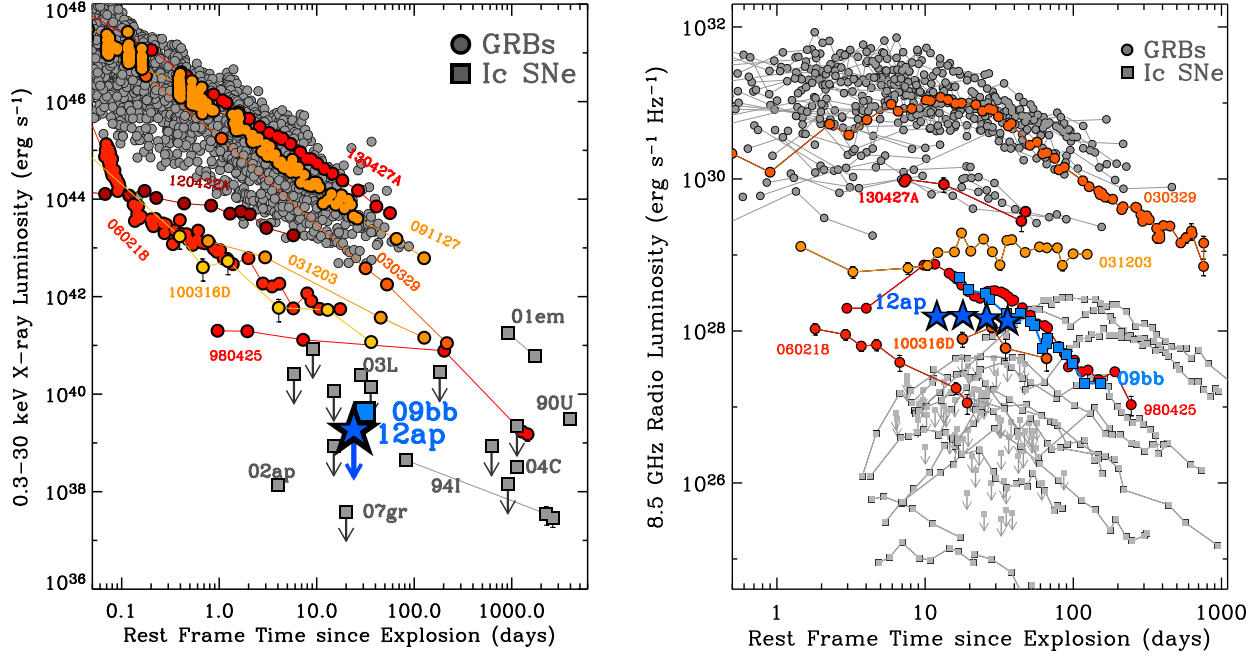


FIG. 3.— *Left panel:* *Chandra* observations put a deep limit to the X-ray luminosity of the relativistic SN 2012ap at  $\sim 20$  days after the explosion. SN 2012ap is considerably less luminous than ordinary long GRBs (filled circles, from Margutti et al. 2013a, Margutti et al. 2013b and referenced therein) and is  $\sim 100$  times fainter than the faintest sub-E GRBs (i.e. GRBs 980425 and 100316D). Filled grey squares: X-ray emission from ordinary Type Ic SNe. The relativistic SN2009bb is marked with a blue square. References: Immler et al. (2002), Pooley & Lewin (2004), Soria et al. (2004), Soderberg et al. (2005), Perna et al. (2008). *Right panel:* radio emission of SN 2012ap (from C14) compared to a sample of GRB radio afterglows (filled circles) and Type Ic SNe (filled square) collected from Soderberg et al. (2010b), Chandra & Frail (2012) and Margutti et al. (2013a). At radio frequencies the luminosity of SN 2012ap is comparable to (or even larger than) sub-E GRBs. In both panels GRBs with spectroscopically associated SNe are in color and labeled.

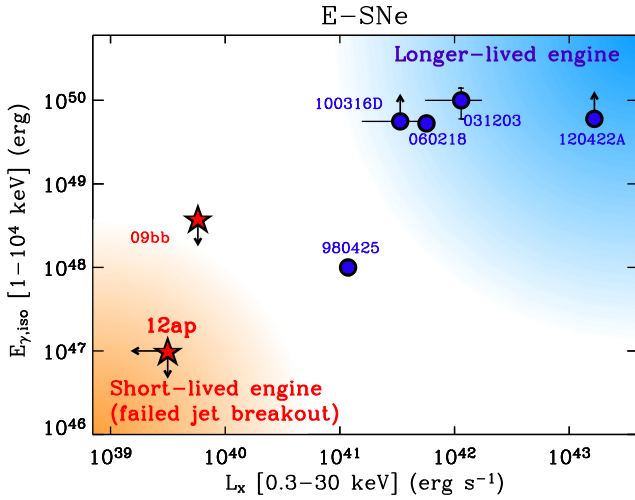


FIG. 4.— Promptly emitted  $\gamma$ -ray energy vs. X-ray luminosity between 10 and 30 days since the explosion for the sample of relativistic SNe (red stars) and sub-E GRBs (blue circles). Relativistic SNe are clearly distinguished from sub-E GRBs by their significantly fainter X-ray emission. References: Amati (2006); Soderberg et al. (2006b); Soderberg et al. (2010b); Starling et al. (2011) Barthelmy et al. (2012); Margutti et al. (2013a); Margutti et al. (2013b); Amati (2013); Amati et al. (2013); C14.

While both relativistic SNe and sub-E GRBs are intermediate between ordinary type Ic SNe and GRBs, our findings point to a diversity in the properties of the progenitors and/or the engines that drive their explosion. This topic is discussed below.

## 5. DISCUSSION

At  $\delta t \gtrsim 10$  d the detected X-ray emission from sub-E GRBs like 060218, 100316D has been shown to originate from

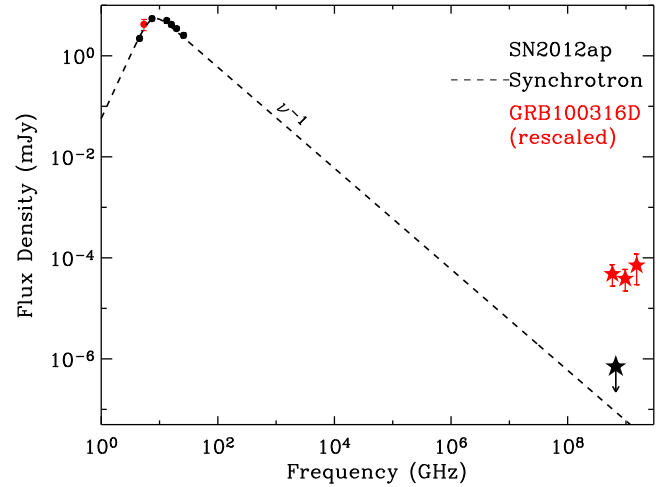


FIG. 5.— Radio (filled black circles) to X-ray (black stars) SED of SN 2012ap. The *Chandra* X-ray upper limit is consistent with the extrapolation of the best-fitting synchrotron model obtained by C14 at  $\delta t \approx 20$  d. Notably, the X-ray emission from SN 2012ap is  $\geq 100$  times fainter than the sub-E GRB 100316D at a similar epoch (here rescaled to match the level of the detected SN 2012ap radio emission), thus ruling out the presence of an extra X-ray component arising from the activity of the explosion central engine.

the activity of the explosion central engine (Soderberg et al. 2006a, Fan & Piran 2006, Margutti et al. 2013a), which dominates over synchrotron emission from the shock-CSM interaction.<sup>10</sup> The nature of the central engine is currently not known. For the sub-E GRBs 060218 and 100316D the obser-

<sup>10</sup> As noted in Margutti et al. (2013a), this extra component might be present in classical GRBs as well, but it is likely out-shined by emission from the the jet-CSM interaction.



vations support either a magnetar central engine or continued accretion onto a newly formed black-hole.

Figure 5 clearly shows that the X-ray emission from SN 2012ap is instead consistent with the shock-CSM model that best fits the radio observations. For SN 2012ap, the deep X-ray limit thus rules out the presence of an additional, luminous X-ray component arising from the engine activity, contrary to sub-E GRBs like 100316D portrayed in Fig. 5. This finding suggests that the engine that powers SN 2012ap is short lived and unable to survive for such a long time.

We propose that relativistic SNe like 2009bb and 2012ap represent the weakest engine-driven explosions, where the engine activity stops before being able to produce a successful jet breakout. The result is a stellar explosion that is able to accelerate a tiny fraction of ejecta to mildly relativistic velocities, thus dynamically different from ordinary Ic SNe and more similar to sub-E and classical GRBs (Fig. 2). In contrast to GRBs, however, the jet is not able to pierce through the stellar envelope, and a very limited fraction of energy is dissipated at  $\gamma$ -ray frequencies, consistent with the deep limit  $E_{\gamma, \text{iso}} < 10^{47}$  erg from C14.

This phenomenology can either be due to an intrinsically short-lived engine or to a different progenitor structure/properties between relativistic SNe and GRBs. In this respect, Lazzati et al. (2012) investigated the role of the duration of the engine activity in stellar explosion induced by relativistic jets with a set of numerical simulations. These authors find that the duration of the engine activity is a key parameter that determines the outcome of a stellar explosion. For a fixed energy budget and progenitor structure, Lazzati et al. (2012) show that the longest-lived engines always produce a successful explosion with a fully relativistic jet (i.e. a classical GRB). Engines with intermediate and short durations (where “short” or “long” is here referred to the time it takes to the jet head to break out through the stellar envelope) would lead instead to partially or totally failed jets, respectively. In particular, relativistic SNe would result from explosions where the engine turns off on the jet breakout time-scale (5–10 s depending on the energy budget and progenitor, Morsony et al. 2007, Lazzati et al. 2012, their Fig. 5), in agreement with our findings of shorter-lived engines.

The failed jet breakout in relativistic SNe can also be due to different progenitor properties compared with sub-E GRBs and ordinary GRBs. To this respect it is relevant to note that the relativistic SNe 2009bb and 2012ap exploded in super-solar and solar metallicity environments, respectively, in line with ordinary Ic SNe (e.g. Sanders et al. 2012; Kelly & Kirshner 2012 and reference therein) but in sharp contrast with sub-E GRBs and classical GRBs that show a marked preference for sub-solar metallicity environments (e.g. Stanek et al. 2006; Margutti et al. 2007; Modjaz et al. 2008; Levesque et al. 2010a). The metallicity of the two relativistic SNe known so far is actually high even compared to the sample of energetic broad-lined Ic SNe *not* connected to GRBs and sub-E GRBs (Sanders et al. 2012; Kelly & Kirshner 2012). For SN 2009bb Levesque et al. (2010b) estimate  $Z = 1.7 - 3.5 Z_{\odot}$ , while for SN 2012ap Milisavljevic et al. (2014) find  $Z = 1.0 Z_{\odot}$ , where solar metallicity  $Z_{\odot}$  corresponds to  $\log(\text{O}/\text{H}) + 12 = 8.69$  (Asplund et al. 2005).

At such high metallicity, line-driven winds in massive stars (e.g. Castor et al. 1975) more efficiently strip away angular momentum from the progenitor through a more sustained mass loss ( $\dot{M} \propto Z^{0.86}$  in Wolf-Rayet stars, likely progenitors

of GRBs, Vink & de Koter 2005).<sup>11</sup> High angular momentum of the progenitor at collapse has been identified by recent numerical simulations (e.g. MacFadyen & Woosley 1999; MacFadyen et al. 2001; Woosley & Heger 2006) as a key physical ingredient of the “collapsar” model to explain the presence of fully relativistic jets in GRBs. It is thus possible that the higher metallicity of the progenitors of relativistic SNe inhibited the formation of a powerful jet able to pierce through the stellar envelope.

The growing sample of GRBs discovered in high-metallicity environments (see e.g. GRBs 050826, 051022 Graham & Fruchter 2013, their Fig. 3 and GRB 120422A, intermediate between ordinary GRBs and sub-E GRBs, Schulze et al. 2014) points however to a more complex situation, where metallicity has some role, but it is unlikely to be the ultimate parameter driving the distribution of angular momentum at collapse.<sup>12</sup> This findings suggest that the higher metallicity of the two known relativistic SNe compared to GRBs might *not* be directly linked to the final explosion outcome. However, it might still indicate a preference for different environments, thus possibly pointing to some relevant difference in their progenitors. In Milisavljevic et al. (2014) we report that both events potentially interacted with carriers of diffuse interstellar bands. This rare phenomenon may also point toward a unique aspect of their progenitor systems.

In addition to extremely small statistics of two objects and differently from GRBs and sub-E GRBs, relativistic SNe were discovered by surveys targeting high mass and hence metal-rich galaxies, so that the higher metallicity of relativistic SNe discussed above may be the result of observational bias. A significantly larger sample of relativistic SNe found through *untargeted* SN searches in the optical and radio band is clearly needed to deeply understand their connection to GRBs, build a complete picture of E-SNe and constrain which unique property differentiates failed breakouts from successful, fully relativistic jets.

## 6. SUMMARY AND CONCLUSIONS

The class of engine-driven SNe (E-SNe) collects a rare variety of SN explosions ( $\lesssim 1\%$  of Type Ic SNe) and includes relativistic SNe, sub-E GRBs and ordinary GRBs. E-SNe are characterized by a significantly shallower kinetic energy profile of the explosion ejecta than expected in the case of a pure hydrodynamic collapse of the progenitor star (Fig. 2), indicating that E-SNe are able to accelerate a tiny but important fraction of their ejecta to higher velocities ( $v \gtrsim 0.6c$ ). E-SNe otherwise show a diverse phenomenology.

Relativistic SNe and sub-E GRBs share a bright radio emission and evidence for mildly relativistic ejecta that clearly set them apart from ordinary SNe Ic (non-relativistic). The thermal properties of relativistic SNe are also analogous to the very energetic, fast expanding SNe associated with sub-E GRBs and ordinary GRBs (Soderberg et al. 2010b, M14). However, a distinctive property of relativistic SNe is their significantly fainter X-ray emission (Fig. 3) that implies the lack of a luminous X-ray component arising from the cen-

<sup>11</sup> Recent findings indicate that episodic mass-loss episodes, as opposed to steady mass-loss through winds, also have a role in the evolution of massive stars. However, the metallicity dependence of these episodes of explosive mass-loss has yet to be constrained. See Margutti et al. (2014) and references therein for details.

<sup>12</sup> A similar conclusion is reached by studies of the close environment of GRBs and energetic broad-lined Ic SNe in the local universe. See Sanders et al. (2012); Kelly et al. (2014).

tral engine activity at late times ( $\delta t \sim 20$  d, Fig. 5). With  $E_{\gamma, \text{iso}} < 10^{47}$  erg, the prompt  $\gamma$ -ray energy released by the relativistic SN 2012ap is also considerably below the level of sub-E GRBs (Fig. 4).<sup>13</sup> The super-solar or solar metallicity of the environment of the two known relativistic SNe also sets them apart from sub-E GRBs and GRBs.

These findings call for some crucial diversity in the properties of the engines and/or of the progenitors of relativistic SNe and sub-E GRBs (and ordinary GRBs as well). We propose that *relativistic SNe represent the weakest engine-driven explosions where the engine is unable to power a successful jet breakout*. This scenario naturally explains (i) the lack of evidence for central engine activity at late times and (ii) the deep limit to the promptly released  $\gamma$ -ray energy.

The failed jet breakout might be due to an intrinsically short-lived engine (but same progenitor properties) or to a different progenitor structure between relativistic SNe and sub-E

GRBs. At the time of writing, with only two relativistic SNe discovered so far (through targeted optical surveys), observations do not allow us to distinguish between these two scenarios. The Large Synoptic Survey Telescope (LSST, Ivezic et al. 2008) is expected to discover hundreds of SNe Ic every year, thus in principle providing the significantly larger sample of E-SNe that is needed to deeply understand the connection between relativistic SNe and GRBs. However, as we demonstrate here, coordinated radio and  $X$ -ray follow up is essential to identify E-SNe from their ordinary counterparts and determine the properties of the engines that power their explosion.

Support for this work was provided by the David and Lucile Packard Foundation Fellowship for Science and Engineering awarded to A. M. S.

## REFERENCES

08. 1  
 Amati, L. 2006, MNRAS, 372, 233  
 Amati, L. 2013, The Astronomical Review, 8, 010000  
 Amati, L., Dichiara, S., Frontera, F., & Guidorzi, C. 2013, GRB Coordinates Network, 14503, 1  
 Asplund, M., Grevesse, N., & Sauval, A. J. 2005, in Astronomical Society of the Pacific Conference Series, Vol. 336, Cosmic Abundances as Records of Stellar Evolution and Nucleosynthesis, ed. T. G. Barnes, III & F. N. Bash, 25  
 Barthelmy, S. D., et al. 2012, GRB Coordinates Network, 13246, 1  
 Björnsson, C.-I., & Fransson, C. 2004, ApJ, 605, 823  
 Bromberg, O., Nakar, E., & Piran, T. 2011, ApJ, 739, L55  
 Burrows, D. N., et al. 2005, Space Sci. Rev., 120, 165  
 Campana, S., et al. 2006, Nature, 442, 1008  
 Castor, J. I., Abbott, D. C., & Klein, R. I. 1975, ApJ, 195, 157  
 Cenko, S. B., et al. 2013, ApJ, 769, 130  
 Chakraborti, S., & Ray, A. 2011, ApJ, 729, 57  
 Chandra, P., & Frail, D. A. 2012, ApJ, 746, 156  
 Chevalier, R. A., & Fransson, C. 2006, ApJ, 651, 381  
 Dessart, L., Burrows, A., Livne, E., & Ott, C. D. 2008, ApJ, 673, L43  
 Fan, Y., & Piran, T. 2006, MNRAS, 369, 197  
 Gehrels, N., et al. 2004, ApJ, 611, 1005  
 Graham, J. F., & Fruchter, A. S. 2013, ApJ, 774, 119  
 Guetta, D., & Della Valle, M. 2007, ApJ, 657, L73  
 Horesh, A., et al. 2013, ApJ, 778, 63  
 Immler, S., Wilson, A. S., & Terashima, Y. 2002, ApJ, 573, L27  
 Ivezic, Z., et al. 2008, ArXiv e-prints  
 Kalberla, P. M. W., Burton, W. B., Hartmann, D., Arnal, E. M., Bajaja, E., Morras, R., & Pöppel, W. G. L. 2005, A&A, 440, 775  
 Kelly, P. L., Filippenko, A. V., Modjaz, M., & Kocevski, D. 2014, ArXiv e-prints  
 Kelly, P. L., & Kirshner, R. P. 2012, ApJ, 759, 107  
 Lazzati, D., Morsony, B. J., Blackwell, C. H., & Begelman, M. C. 2012, ApJ, 750, 68  
 Levesque, E. M., Kewley, L. J., Berger, E., & Zahid, H. J. 2010a, AJ, 140, 1557  
 Levesque, E. M., et al. 2010b, ApJ, 709, L26  
 MacFadyen, A. I., & Woosley, S. E. 1999, ApJ, 524, 262  
 MacFadyen, A. I., Woosley, S. E., & Heger, A. 2001, ApJ, 550, 410  
 Margutti, R., et al. 2007, A&A, 474, 815  
 Margutti, R., et al. 2014, ApJ, 780, 21  
 Margutti, R., et al. 2012, ApJ, 751, 134  
 Margutti, R., et al. 2013a, ApJ, 778, 18  
 Margutti, R., et al. 2013b, MNRAS, 428, 729  
 Matzner, C. D., & McKee, C. F. 1999, ApJ, 510, 379  
 Milisavljevic, D., et al. 2014, ApJ, 782, L5  
 Modjaz, M., et al. 2008, AJ, 135, 1136  
 Morsony, B. J., Lazzati, D., & Begelman, M. C. 2007, ApJ, 665, 569  
 Nakar, E., & Sari, R. 2012, ApJ, 747, 88  
 Paragi, Z., et al. 2010, Nature, 463, 516  
 Perna, R., Soria, R., Pooley, D., & Stella, L. 2008, MNRAS, 384, 1638  
 Pooley, D., & Lewin, W. H. G. 2004, IAU Circ., 8323, 2  
 Predehl, P., & Schmitt, J. H. M. M. 1995, A&A, 293, 889  
 Sanders, N. E., et al. 2012, ApJ, 758, 132  
 Schulze, S., et al. 2014, ArXiv e-prints  
 Soderberg, A. M., et al. 2006a, ApJ, 650, 261  
 Soderberg, A. M., Brunthaler, A., Nakar, E., Chevalier, R. A., & Bietenholz, M. F. 2010a, ApJ, 725, 922  
 Soderberg, A. M., et al. 2010b, Nature, 463, 513  
 Soderberg, A. M., Kulkarni, S. R., Berger, E., Chevalier, R. A., Frail, D. A., Fox, D. B., & Walker, R. C. 2005, ApJ, 621, 908  
 Soderberg, A. M., et al. 2006b, Nature, 442, 1014  
 Soria, R., Pian, E., & Mazzali, P. A. 2004, A&A, 413, 107  
 Springob, C. M., Masters, K. L., Haynes, M. P., Giovanelli, R., & Marinoni, C. 2007, ApJS, 172, 599  
 Springob, C. M., Masters, K. L., Haynes, M. P., Giovanelli, R., & Marinoni, C. 2009, ApJS, 182, 474  
 Stanek, K. Z., et al. 2006, Acta Astron., 56, 333  
 Starling, R. L. C., et al. 2011, MNRAS, 411, 2792  
 Tan, J. C., Matzner, C. D., & McKee, C. F. 2001, ApJ, 551, 946  
 Vink, J. S., & de Koter, A. 2005, A&A, 442, 587  
 Watson, D. 2011, A&A, 533, A16  
 Woosley, S. E., & Heger, A. 2006, ApJ, 637, 914

<sup>13</sup> For the other relativistic SN 2009bb the observational limit on the

promptly released  $E_{\gamma, \text{iso}}$  is unfortunately not as constraining (Fig. 4).